

Influence of Flexible Spacers on Liquid-Crystalline Self-Assembly of T-Shaped Bolaamphiphiles

Xiaohong Cheng,^{*,†,‡} Feng Liu,[§] Xiangbing Zeng,[§] Goran Ungar,^{*,§,⊥} Jens Kain,^{||} Siegmund Diele,^{||} Marko Prehm,^{‡,||} and Carsten Tschierske^{*,‡}

[†]Department of Chemistry, Key Laboratory of Medicinal Chemistry for Natural Resources (Ministry of Education), Yunnan University, Kunming, Yunnan 650091, P. R. China

[‡]Organic Chemistry and ^{||}Physical Chemistry, Institute of Chemistry, Martin-Luther University Halle-Wittenberg, D-06120 Halle, Germany

[§]Department of Materials Science and Engineering, University of Sheffield, Mappin Street, Sheffield S13JD, U.K.

[⊥]WCU program Chemical Convergence for Energy and Environment, School of Chemical and Biological Engineering, Seoul National University, Seoul, Korea

S Supporting Information

ABSTRACT: T-shaped bolaamphiphiles composed of a biphenyl rigid core, a semiperfluorinated lateral chain, two polar 1,2-diol groups in the terminal positions and flexible alkyl spacers connecting the polar groups with the biphenyl core have been synthesized and investigated by polarizing microscopy, DSC and X-ray scattering. The influence of spacer length and position of the spacer on the self-assembly in liquid-crystalline phases was studied. A series of four different columnar phases ($Col_{hex}/p6mm$, $Col_{rec}/p2gg$, $Col_{squ}/p4gm$ and $Col_{squ}/p4mm$), representing liquid-crystalline honeycomb structures composed of cylinders having hexagonal, pentagonal, and square cross section, were found on increasing the spacer length. It is also shown that introduction of aliphatic spacers in the backbone of the T-shaped bolaamphiphiles replaces the $Col_{rec}/c2mm$ phase made up of rhombic cylinders with the $Col_{squ}/p4mm$ phase composed of square cylinders. It also causes the 2d lattice of pentagonal cylinders to increase the symmetry from $Col_{rec}/p2gg$ to $Col_{squ}/p4gm$. A temperature-dependent second-order phase transition between these two pentagonal cylinder structures was observed for the first time. Beside these effects on cylinder shape and phase symmetry the flexible spacer units also lead to reduced phase transition temperatures and allow adjustment of cylinder side length to envelop a wider range of side-chain sizes. Electron density maps suggest that this may involve sacrificing some of the hydrogen bonds.



1. INTRODUCTION

The investigation of molecular self-assembly is one of the most exciting areas of contemporary chemical research.¹ Liquid-crystalline (LC) systems^{2,3} combine order and mobility and therefore can be regarded as simple model systems in which the driving forces of self-assembly at the nanoscale level can be studied in a systematic and controlled manner.⁴ LC dendrimers^{5,6} and supermolecules,⁷ chirality-induced LC superstructures,⁸ formation of ferroelectric organic materials and spontaneous achiral symmetry breaking in mesophases formed by bent-core molecules,⁹ as well as LC magnets¹⁰ and liquid quasicrystals¹¹ are selected topics of contemporary research in this rapidly developing field.

Based on the concept of competitive polyphilicity, it was also possible to increase the complexity of LC phases considerably.^{12–16} This concept was successfully applied to two types of T-shaped ternary amphiphiles incorporating a rigid rodlike core, namely bolaamphiphiles^{12,13,15,17} and facial amphiphiles.^{15,18} A major group of LC phases formed by these polyphilic tectons represent

polygonal cylinder phases. In these soft honeycomb structures the rodlike cores organize into cylinder frameworks, held together by attractive interactions between the terminal groups located at the edges of the cylinder walls and the resulting cells are filled with the disordered lateral chains.¹⁵ In these structures the length of the rigid core with respect to the volume of the lateral chains determines the number of rodlike cores organized in the circumference of the cylinders. In this way, increasing the volume of the lateral chains at constant core length leads to a series of cylinder structures starting with rhombuses, followed by pentagons, regular and stretched hexagons,¹⁹ and ending with giant pentagons (Figure 1c–g),^{12,15} followed by a bursting of these cylinders^{17b} with formation of a new kind of lamellar phases (Lam, Figure 1h–k).²⁰

For the series of bolaamphiphilic biphenyl derivatives with lateral alkyl (Hm-1/1) or semiperfluoroalkyl substituents

Received: January 27, 2011

Published: May 02, 2011

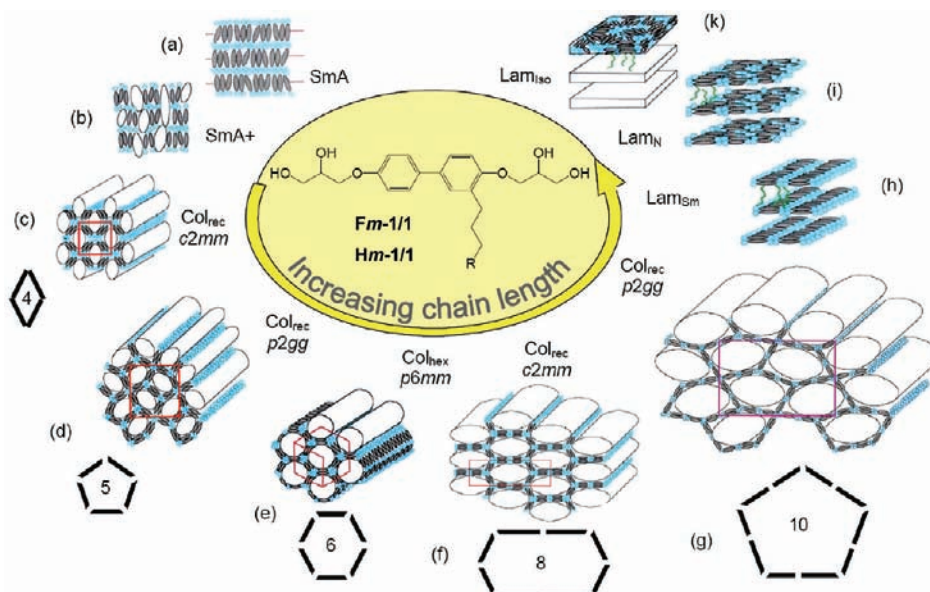


Figure 1. Mesophases reported for calamitic biphenyl-based bolaamphiphiles with nonpolar (alkyl or semiperfluoroalkyl) lateral chains in the peripheral 3-position; compounds **Fm-1/1**: $R = C_mF_{2m+1}$; compounds **Hm-1/1**: $R = C_mH_{2m+1}$; abbreviations: SmA = smectic A phase; Col_{rec} = rectangular columnar phase; Col_{squ} = square columnar phase; Col_{hex} = hexagonal columnar phase; Lam_{Iso}, Lam_N, Lam_{Sm}, laminated phases with different orders of the rodlike units in the layers.¹⁵

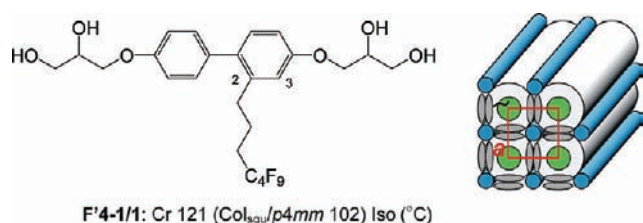
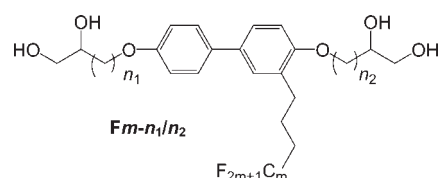


Figure 2. Molecular structure, transition temperatures ($T/^\circ\text{C}$), and molecular self-assembly of compound **F'4-1/1** in its Col_{squ}/p4mm type liquid-crystalline phase; the brackets indicate that the Col_{squ}/p4mm phase is monotropic and can only be observed on cooling from the isotropic liquid state.¹³

(**Fm-1/1**), shown in Figure 1, a transition from the SmA phase via a *c2mm*-type rectangular columnar phase composed of rhombic cylinders (Figure 1c) to a pentagonal cylinder phase with *p2gg* symmetry (Figure 1d) was observed as the first steps upon elongation of the lateral chain (increasing m).^{12,13} The *c2mm* phase (Figure 1c) can be regarded as a slightly distorted version of the square cylinder phase (Col_{squ}/p4mm, see Figure 2, right) with angles unequal to 90° . The nondistorted p4mm phase was observed for ternary T-shaped polyphiles with longer aromatic cores, such as *p*-terphenyls,^{18,21} diphenylthiophenes²² and even longer rodlike cores.^{23,24} For the biphenyl derivatives, only in one exceptional case a short monotropic (metastable) region of the square cylinder phase (Col_{squ}/p4mm) could be achieved after shifting the position of the lateral chain from the peripheral 3-position to the more central 2-position (compound **F'4-1/1** in Figure 2).^{13,25} Hence, it appears that the distance between lateral chain and polar groups decides whether cylinders with a square or a rhombic cross section are formed.

Here we report new T-shaped bolaamphiphiles with a semi-perfluorinated lateral chain but having an additional aliphatic spacer between the rigid aromatic core and the polar groups.

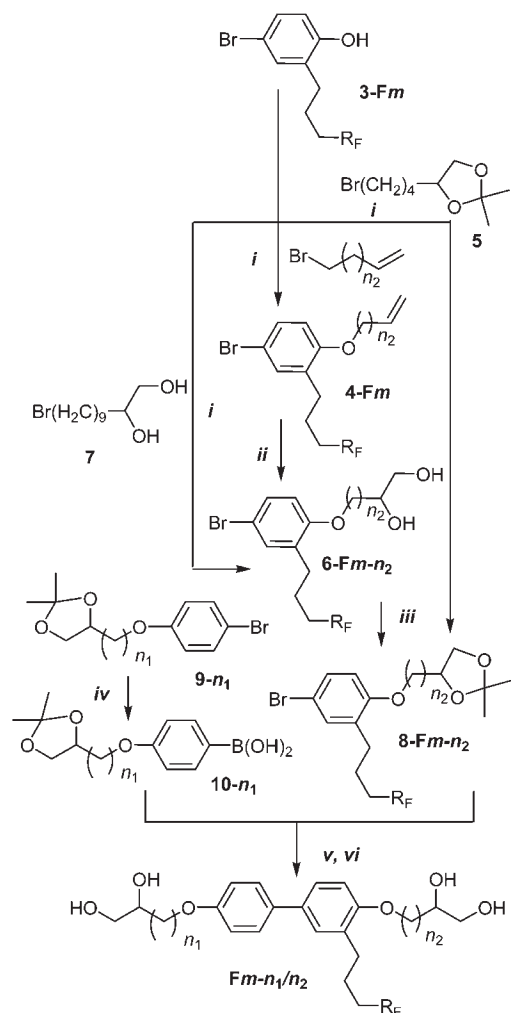
Chart 1. Structure and Designation of the Molecules under Investigation



Furthermore, the influence of spacer length and position on the mode of LC self-assembly is discussed. In the compounds denoted **Fm- n_1/n_2** , m indicates the number of CF_2 groups in the lateral chain and n_1/n_2 give the spacer lengths used to couple the 1,2-diol units to the two different ends of the biphenyl core (see Chart 1). It is shown that with increasing spacer length (n_1, n_2), rhombic cylinders are replaced by square cylinders, resulting in the following sequence of four distinct honeycomb LC phases: Col_{hex}/p6mm (hexagons) – Col_{rec}/p2gg (pentagons), Col_{squ}/p4gm (pentagons) – Col_{squ}/p4mm (squares). Moreover, for the first time a temperature-induced transition between two pentagonal cylinder phases with symmetries *p2gg* and *p4gm* was observed in one of the compounds.

2. RESULTS AND DISCUSSION

2.1. Synthesis. Bolaamphiphiles **Fm- n_1/n_2** were prepared as shown in Scheme 1 using Suzuki coupling reactions²⁶ as key steps. The 4-bromophenols **3-Fm** ($m = 6, 8$) with perfluorinated lateral chains attached via a propylene spacer to the 2-position were synthesized by Pd⁰-catalyzed addition of 1-iodoperfluoroalkanes to 2-allylphenol,²⁷ followed by para-selective bromination using HBr/AcOH/DMSO.²⁸ Starting with compounds **3-Fm** the building blocks **8-Fm- n_2** ($m = 6, 8$ and $n_2 = 1, 4, 9$) were produced in three different ways. Etherification of the

Scheme 1. Synthesis of Bolaamphiphiles $Fm-n_1/n_2$ ^a

^a Reagents and conditions: i) K_2CO_3 , CH_3CN , reflux, 6 h (80–93%). ii) OsO_4 , *N*-methylmorpholine-*N*-oxide, H_2O , acetone, 25 °C (52–66%). iii) $Me_2C(OMe)_2$, Py, TosOH, CH_2Cl_2 , 25 °C, 24 h (73–93%). iv) 1. *n*-BuLi, –100 °C; 2. $B(OMe)_3$; 3. phosphate buffer, 0 °C (43–60%). v) $Pd(PPh_3)_4$, $NaHCO_3$, glyme, H_2O , reflux, 6 h (25–92%). vi) 10% HCl, EtOH, 25 °C, 24 h (90–95% crude products, 12–22%, after all purification steps).

4-bromophenols **3-Fm** with 4-(4-bromobutyl)-2,2-dimethyl-1,3-dioxolane **5**²⁹ afforded compounds **8-Fm-4** with butylene spacer. Etherification of the 4-bromophenols **3-Fm** with 11-bromo-undecane-1,2-diol **7** gave the substituted 11-(4-bromophenoxy)undecane-1,2-diols **6-Fm-9** in the first step. Protection of the diol groups of the obtained compounds **6-Fm-9** using 2,2-dimethoxypropane and catalytic amounts of pyridinium tosylate produced the bromoarenes **8-Fm-9** with the longest spacer unit ($n_2 = 9$).³⁰ For the preparation of the bromoarenes **8-Fm-1** with the shortest spacers, we used the etherification of 4-bromophenols **3-Fm** first with allylbromide, followed by dihydroxylation of the double bond with osmium-tetroxide/*N*MMNO (*N*-methylmorpholine-*N*-oxide) in an acetone/water mixture,³¹ and protection of the diol group as the final step. The glycerol functionalized benzene boronic acids **10-n₁** ($n_1 = 1, 4$) were prepared by halogen/metal exchange reaction of the arylbromides **9-n₁**³² with *n*-butyllithium at –100 °C followed

by quenching with trimethylborate at –90 °C. Hydrolysis to the boronic acids **10-n₁** was carried out at 0 °C using phosphate buffer adjusted to pH = 4.5–5.¹² The coupling reactions of the boronic acids **10-n₁** with the appropriate aryl bromides **8-Fm-n₂** were carried out using standard conditions with $Pd(PPh_3)_4$, in aqueous glyme and $NaHCO_3$ as base. In the final step, the acetonide groups were cleaved (HCl in EtOH) and the bolaamphiphiles **Fm-n₁/n₂** were purified by repeated crystallization. Detailed synthetic procedures and analytical data are given in the Supporting Information (SI).

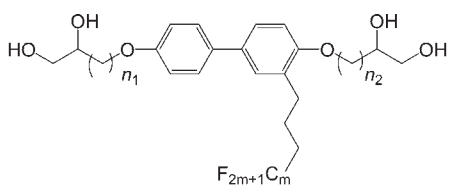
2.2. Methods of Investigation and General Trends. Compounds **Fm-n₁/n₂** were investigated by polarized optical microscopy (POM; Optiphot 2, Nikon in conjunction with a heating stage FP 82 HT, Mettler), differential scanning calorimetry (DSC; DSC-7, Perkin-Elmer), and X-ray diffraction (XRD) of powder samples and surface aligned samples. Investigations of surface aligned samples were performed using a 2D detector (HI-Star, Siemens). Uniform orientation was achieved by slowly cooling a drop of the compound on a glass surface. The X-ray beam was applied parallel to the substrate (exposure time: between 30 min and 3 h).

Two series of compounds were prepared and investigated, series **F6-n₁/n₂** with a C_6F_{13} perfluorinated segment, and series **F8-n₁/n₂** with a C_8F_{17} segment, attached to the lateral chain. The phase transition temperatures and corresponding enthalpy values for both series are collated in Table 1, together with other data. All compounds form broad regions of enantiotropic (thermodynamically stable) liquid-crystalline phases. In the mesomorphic temperature ranges the X-ray diffraction patterns show a broad diffuse wide angle scattering with maxima at $d = 0.52$ nm for compounds **F6-n₁/n₂** (Figure 3g) and at $d = 0.54$ nm for compounds **F8-n₁/n₂** (Figure S6e, SI) confirming the LC nature of all mesophases. This diffuse scattering has a ring-like shape and the rather large d -value of the maxima indicate that the R_F segments significantly contribute to this scattering. Indexing of the small-angle Bragg reflections (see Table S1 in SI) leads to the phase assignments with plane groups shown in Table 1.

2.3. Effect of Spacer Length on Mesomorphic Self-Assembly in the Series of Compounds F6-n₁/n₂. For the series of compounds **F6-n₁/n₂** with the shorter fluorinated segment four distinct types of columnar phases were observed depending on the spacer length, the distribution of the spacers along the lipophilic core moiety and temperature. The columnar phase of compound **F6-1/1** with two glycerol-type polar end groups ($n_1, n_2 = 1$) was previously reported as a hexagonal columnar phase composed of an array of hexagonal cylinders (see Table 1 and Figure 1e).¹³

Compound **F6-1/4** is obtained by increasing the length (n_2) of the spacer adjacent to the benzene ring carrying the R_F chain to $n_2 = 4$. For this compound a birefringent texture appears at $T = 143$ °C on cooling from the isotropic liquid. This texture, shown in Figure 3a, is typical of a columnar phase, characterized by birefringent domains and homeotropically aligned areas which appear completely dark, indicating that this mesophase is optically uniaxial. Investigation with a λ -retarder plate (Figure 3c) leads to the conclusion that this mesophase is optically negative,³⁴ like those of all **Fm-n₁/n₂** compounds. This means that the major intramolecular π -conjugation pathway along the long axis of the biphenyl cores is perpendicular to the column long axis. This mesogen orientation is common to most polygonal cylinder phases. On further cooling (at $T = 129$ °C) weak birefringence appears in the homeotropically aligned regions.

Table 1. Transition Temperatures, Associated Enthalpy Values (lower lines, in italics) and Lattice Parameter and Other Data of the T-Shaped Bolaamphiphiles $Fm-n_1/n_2$.^a



Compd.	<i>m</i>	<i>n</i> ₁	<i>n</i> ₂	<i>L</i> _{mol} /nm	<i>T</i> /°C <i>ΔH</i> /KJ mol ⁻¹	<i>a, b</i> /nm	<i>n</i> _{cell}	Polygon	<i>n</i> _{wall}
F6-1/1 ¹³	6	1	1	2.1	Cr 47 Col _{hex} / <i>p6mm</i> 171 Iso <i>12.4</i> <i>8.5</i>	<i>a</i> = 3.47	5.9	hex	2.0
F6-1/4	6	1	4	2.5	Cr 94 Col _{rec} / <i>p2gg</i> 129 Col _{rec} / <i>p4gm</i> 143 Iso <i>5.1</i> - <i>4.3</i>	<i>a</i> = 6.18 ^b <i>a</i> = 6.47 ^c , <i>b</i> = 6.00 ^c	19.5 ^b 19.9 ^c	pent pent	2.0 ^b 2.0 ^c
F6-1/9	6	1	9	3.2	Cr 71 Col _{squ} / <i>p4mm</i> 116 Iso <i>33.6</i> <i>2.6</i>	<i>a</i> = 2.94	3.9	squ	2.0
F6-4/4	6	4	4	3.1	Cr 55 Col _{squ} / <i>p4mm</i> 102 Iso <i>14.8</i> <i>3.4</i>	<i>a</i> = 3.00	4.2	squ	2.1
F8-1/1 ¹³	8	1	1	2.1	Cr 70 Col _{hex} / <i>p6mm</i> 188 Iso <i>5.3</i> <i>9.3</i>	<i>a</i> = 3.61	5.8	hex	1.9
F8-4/1	8	4	1	2.5	Cr 70 Col _{hex} / <i>p6mm</i> 138 Iso <i>18.5</i> <i>5.4</i>	<i>a</i> = 4.05	6.6	hex	2.2
F8-1/4	8	1	4	2.5	Cr 84 Col _{hex} / <i>p6mm</i> 159 Iso <i>18.0</i> <i>6.4</i>	<i>a</i> = 4.07	6.7	hex	2.2
F8-1/9	8	1	9	3.2	Cr 93 (M 58) Col _{squ} / <i>p4mm</i> 136 Iso <i>26.4</i> <i>0.6</i> <i>4.7</i>	<i>a</i> = 3.19	4.1	squ	2.1

^a Transition temperatures were determined by DSC (peak temperatures, first heating scan, 10 K min⁻¹); *L*_{mol} = molecular length as measured between the ends of the primary OH groups at both ends in the most extended conformation of the molecules (CPK models); *n*_{cell} = number of molecules in the unit cell, calculated using the crystal volume increments of Immirzi³³ as described in the SI (Table S2); “polygon” describes the shape of the cylinder cross section; *n*_{wall} = average thickness of the cylinder walls given by the average number of biphenyl units arranged side by side in the walls separating two adjacent cylinder cores, calculated by dividing *n*_{cell} by the number of cylinder walls in the unit cell, i.e. for Col_{squ}/*p4mm*, *n*_{cell} is divided by 2, for Col_{hex}/*p6mm* by 3, and for Col_{rec}/*p2gg*/Col_{squ}/*p4gm* by 10; abbreviations: Cr = crystalline solid, Col_{squ}/*p4mm* = square columnar phase with *p4mm* lattice (square honeycomb), Col_{hex}/*p6mm* = hexagonal columnar phase with *p6mm* lattice (hexagonal honeycomb), Col_{squ}/*p4gm* = square columnar phase with *p4gm* lattice, Col_{rec}/*p2gg* = rectangular columnar mesophase with *p2gg* lattice (pentagonal honeycombs), M = unknown mesophase, Iso = isotropic liquid. ^b Values for Col_{squ}/*p4gm* phase at *T* = 130 °C. ^c Values for Col_{rec}/*p2gg* phase at *T* = 120 °C.

The birefringence increases continuously upon further cooling, and a birefringent stripy pattern develops (Figure 3b). At this transition the orientation of the columns does not change (compare c and d of Figure 3) and there is no associated enthalpy change (Figure 3h), which suggests a second-order or only weakly first-order phase transition.

Small angle XRD patterns of an aligned sample recorded at *T* = 130–135 °C can be indexed on a square lattice with *p4gm* symmetry (see Figure 3e; *a*_{squ} = 6.2 nm at *T* = 130 °C). This changes below 130 °C to a rectangular lattice with *p2gg* symmetry and parameters *a* = 6.5 nm and *b* = 6.0 nm at *T* = 120 °C (see Figure 3f and Tables S1, S2 in SI). In previously reported T-shaped amphiphiles the columnar phases with *p4gm* lattice were found to display two different honeycomb structures, one combining square and triangular cylinders in a 1:2 ratio, and the other consisting of pentagonal cylinders only.^{18c} The triangle-square structure can be excluded for the present case since the *p4gm* phase of **F6-1/4** changes into a hexagonal cylinder phase if the length of the bolaamphiphilic core is reduced by decreasing the spacer length (compound **F6-1/1**) and to a square cylinder phase if the bolaamphiphilic core is enlarged by increasing the

spacer length (compounds **F6-4/4** and **F6-1/9**, see Table 1). It follows that the cylinders forming the *p4gm* phase of compound **F6-1/4** must have a shape between square and hexagon but not triangle, which therefore excludes the triangle-square tiling. Hence, the present *p4gm* phase is likely to represent an array of cylinders with pentagonal cross section made up of five aromatic cores in circumference. The cylinders are grouped in pairs and arranged in a herringbone pattern. The electron density map (Figure 3i) reconstructed from the diffraction intensities (Figure 3e) shows a cut through this cylinder structure. The high electron density areas (blue, purple) indicate the position of the columns incorporating the R_F segments of the lateral chains and in the green shells the alkyl parts of the lateral chains are partly mixed with the R_F chains. These high electron density areas are centered in the pentagonal cylinder cells; the low electron density areas (red, yellow) mark the positions of the polar (diol) columns and spacer units. The superimposed black lines indicate the average positions of the biphenyls interconnecting these polar columns. The pentagons are not regular, as regular pentagons cannot tile a plane. The *p2gg* phases of T-shaped bolaamphiphiles are also known to consist of pentagonal

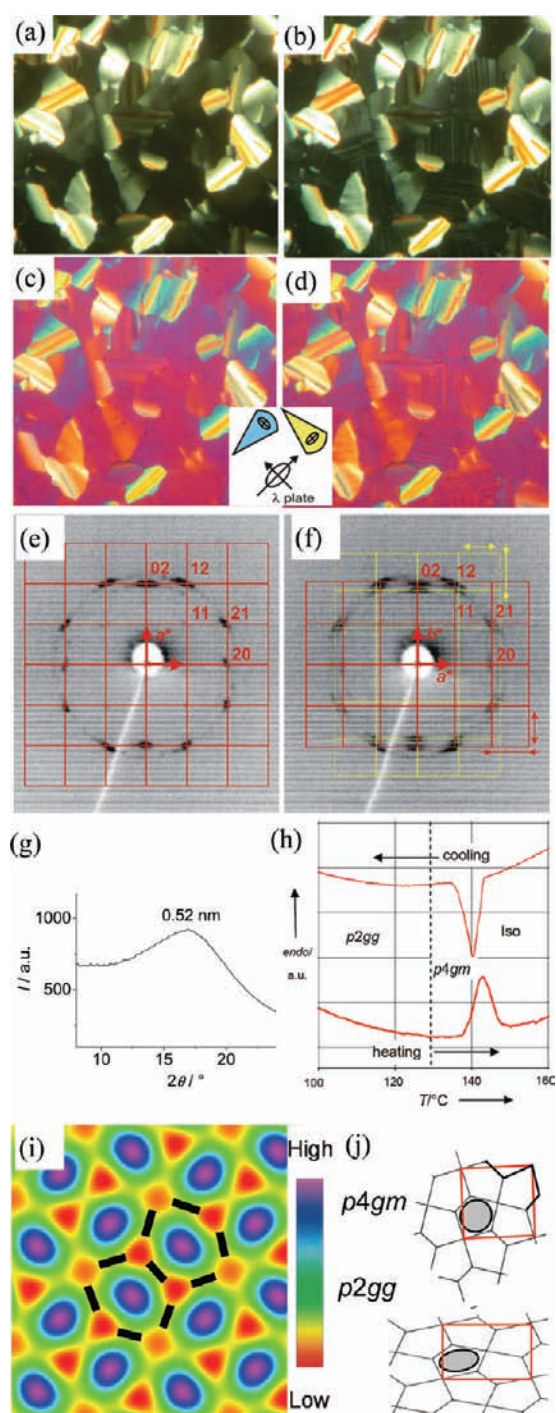


Figure 3. Compound F6-1/4. (a) Texture as seen between crossed polarizers in the Col_{squ}/p4gm phase at $T = 132$ °C; (b) in the Col_{rec}/p2gg phase $T = 60$ °C; (c) texture of the Col_{squ}/p4gm and (d) Col_{rec}/p2gg phase with λ -retarder plate (same areas and temperatures; the indicatrix orientation in the compensator is shown in the inset); (e) X-ray diffraction pattern of an aligned sample in the Col_{squ}/p4gm phase at $T = 132$ °C and (f) of the Col_{rec}/p2gg phase at $T = 60$ °C; (g) scan over the wide angle region at $T = 120$ °C; (h) DSC heating and cooling scans (10 K min^{-1}) in the temperature range of the p2gg-p4gm-Iso phase transition; (i) electron density map as calculated for the p4gm phase from the diffraction pattern at $T = 132$ °C; for color code, see bar on the right; the positions of the bolaamphiphilic moieties are indicated by the dark lines (relative Bragg diffraction intensities used: $I_{11} = 4.2$, $I_{20} = 68$, $I_{21} = 100$, respective phase angles π , π , 0); and (j) comparison of the p4gm and p2gg lattices.

cylinders, but the pentagons are even more distorted than in the p4gm phase (see Figure 3j).¹³ An estimate of the number n_{cell} of molecules in each hypothetical unit cell with an assumed height of $h = 0.45$ nm was obtained by comparing the unit cell volume with the molecular volume as calculated from volume increments³³ (the reason for choosing $h = 0.45$ nm is explained in a footnote³⁵ and for details of the calculations, see Table S2 in SI). The resulting values are $n_{\text{cell}} = 19-20$ and $n_{\text{cell}} = 20$ for the p4gm and p2gg phases, respectively. These values are in good agreement with those previously reported for pentagonal cylinder phases of other compounds.^{13,18c,18d,22} Considering there are 10 cylinder walls in a unit cell the above n_{cell} values indicate that the walls are formed by two aromatic cores arranged side-by-side ($n_{\text{wall}} = 1.9-2.0$).

It is a characteristic of second-order phase transitions that there are sizable fluctuations on both sides of the transition temperature T_c . Thus just above T_c the square phase is expected to contain local domains of the rectangular p2gg phase with equal probability of the long rectangle axis being aligned along x_1 and x_2 axes of the p4gm square lattice. Similarly, just below T_c there are local domains of the rectangular p2gg phase oriented perpendicular to the dominant direction elsewhere in the lattice. As a result, upon cooling a uniformly aligned sample of the p4gm phase (Figure 3e), the p2gg phase forms as a domain structure composed of two nearly equally populated domains aligned in mutually perpendicular directions (Figure 3f). Ease of deformation of the pentagonal cylinders should lower the energy of the domain boundaries and thus facilitate the formation of the entropically favored square phase at elevated temperature. It is therefore not surprising that the transition between the p2gg and p4gm pentagonal cylinder phases is observed here for the first time; the long spacer as part of the molecular backbone allows flexibility in wall length, which lowers the energy of the domain boundaries. In contrast, the related compounds Fm-1/1 without long spacers form exclusively the p2gg pentagonal honeycomb. Hence, it seems that increasing the distance between aromatic core and polar diol group provides flexibility necessary to achieve high-entropy high-symmetry phases.²² It is also worth pointing out that in facial amphiphiles, which have a polar oligo-(oxyethylene) side-chain and two flexible terminal alkyl chains, pentagonal cylinders were only ever found to form the p4gm phase, and never the p2gg.^{18a,c,d}

This, however, does not mean that the backbone flexibility is the only factor bringing about the p4gm phase. There are several other factors. The first is the tendency of the linear R_F chain segments for parallel alignment which favors stretched pentagons, destabilizing p4gm and favoring p2gg symmetry at lower temperatures. The more flexible oligo-(oxyethylene) side chain of the above-mentioned facial amphiphiles^{18c,d} easily fill the “p4gm-pentagons” and therefore do not require cell deformation. Additional factors favoring the p4gm phase are a more central position of the lateral chain which allows an easier filling of the more circular area inside “p4gm-pentagons” and the correct ratio of cube root of side-chain volume to backbone length.

Compound F6-1/9 with the longest spacer between biphenyl core and the diol group ($n_2 = 9$) displays a square columnar phase as indicated by the ratio of $\sin\theta$ of the small angle reflections being $1:\sqrt{2}$ (see Table 1; Table S1 in the SI). On the basis of the 2d XRD pattern obtained for an aligned sample this square phase can be assigned to a simple square lattice with plane group p4mm (Figure S3a–c, SI). The lattice parameter $a_{\text{squ}} = 2.94$ nm is close to the molecular length ($L_{\text{mol}} = 3.2$ nm). This is in agreement with a square honeycomb structure (see Figure 2, right), which is

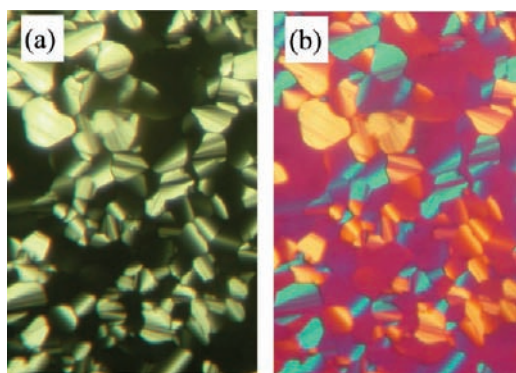


Figure 4. Texture as seen for $\text{Col}_{\text{squ}}/p4mm$ phase of compound **F6-1/9** (a) between crossed polarizers at $T = 115\text{ }^\circ\text{C}$, the dark areas are homeotropically aligned regions; (b) texture with λ -plate (same area), the indicatrix orientation in the compensator is the same as shown in the inset in Figure 3c,d.

also in line with the lack of birefringence for light traveling along the columns in the homeotropic areas (Figure 4a) and the negative birefringence in other areas (see Figure 4b).

The phase sequence $\text{Col}_{\text{hex}}/p6mm$ (hexagons) – $\text{Col}_{\text{rec}}/p2gg$ / $\text{Col}_{\text{squ}}/p4gm$ (pentagons) – $\text{Col}_{\text{squ}}/p4mm$ (squares) as observed upon increasing the spacer length n_2 indicates that extending the spacer has the same effect as reducing the length of the lateral chains (see Figure 1). In the series of compounds **F6-1/ n_2** , by increasing n_2 from 1 via 4 to 9, the length of the side of the polygon increases while the volume (area) required by the lateral chains remains constant. Therefore, fewer cores are required to enclose the semiperfluorinated lateral chains, and the number of sides of the polygon decreases (Table 1).

F6-4/4 is different from the compounds discussed so far, as in this compound two equally long spacers separate the biphenyl core from the terminal polar groups. XRD patterns of compounds **F6-4/4** and **F6-1/9** are both indexed on a square lattice with $p4mm$ symmetry (see Figures S4a and S4f,g, SI). For **F6-4/4**, the phase structure was further corroborated by electron density reconstruction. The electron density map obtained from Bragg peak intensities of the small angle synchrotron powder pattern (Figure S4g, Table S3a in SI) is shown in Figure 5c. The maximum (A) is due to the perfluorinated lateral chains in the center of the honeycomb cell. Perfluorinated alkyl is known to have a far higher electron density than the rest of the molecule; for the molecular model of this phase see Figure 5e.

The lattice parameter a_{squ} is slightly larger for **F6-4/4** ($a_{\text{squ}} = 3.0\text{ nm}$) than for **F6-1/9** ($a_{\text{squ}} = 2.9\text{ nm}$), although **F6-4/4** ($L_{\text{mol}} = 3.1\text{ nm}$) has a total spacer length two CH_2 units shorter than **F6-1/9** ($L_{\text{mol}} = 3.2\text{ nm}$). This suggests that a longer and thus more flexible alkylene spacer at only one end (compound **F6-1/9**) allows more efficient space filling. In principle, there are three possible arrangements of the bolaamphiphilic cores in the cylinder walls, either with segregation of the biphenyls from the alkylene spacers (parallel alignment as in Figure 5f), a nonsegregated structure with antiparallel side-by-side organization of the bolaamphiphilic cores or a randomly mixed structure. It is reasonable to assume that the flexible alkylene spacers segregate from the rigid biphenyls¹⁴ as in Figure 5f. However, there is no indication of a long-range ordered super lattice with reduced symmetry and long-range order of the segregated aromatic and aliphatic regions of compound **F6-1/9** in the cylinder walls. Therefore, it appears

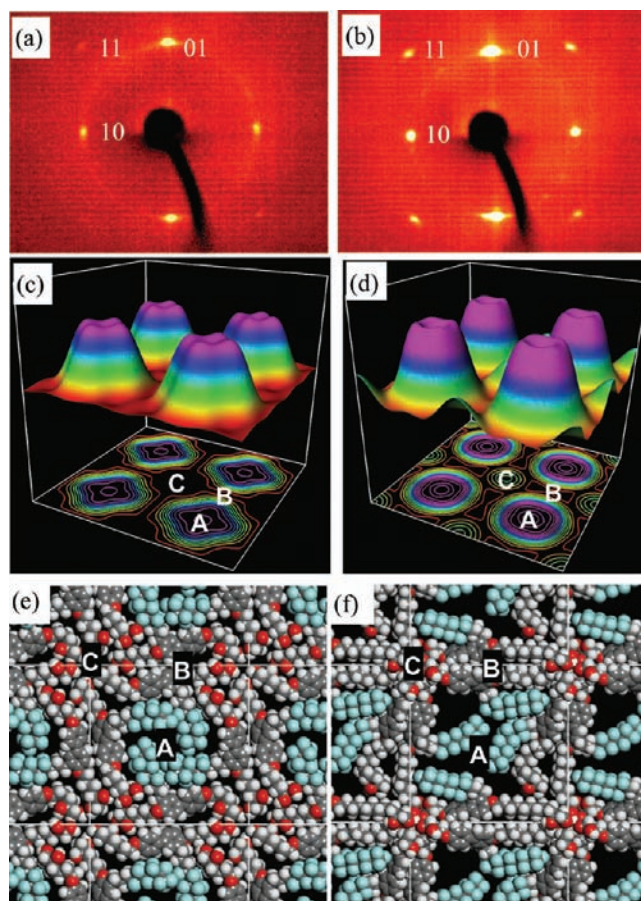


Figure 5. $\text{Col}_{\text{squ}}/p4mm$ phases of compounds **F6-4/4** (left) and **F8-1/9** (right): (a) X-ray diffraction pattern of an aligned sample (small angle region) of compound **F6-4/4** at $90\text{ }^\circ\text{C}$ and (b) **F8-1/9** at $97\text{ }^\circ\text{C}$; (c,d) electron density maps (surface and contour plots, four unit cells) as calculated from the synchrotron powder SAXS data for (c) compound **F6-4/4** (see Figure S4g in SI) and (d) compound **F8-1/9** (see Figure S7d in SI); see SI for details on map construction and related 2d presentations (Figure S1 in SI); (e,f) arrangement of molecules in the $\text{Col}_{\text{squ}}/p4mm$ phases of (e) compound **F6-4/4** and (f) compound **F8-1/9** after molecular dynamic simulation (for details see SI).

reasonable that core orientation in the cylinder walls is on a larger scale averaged, resulting in overall $p4mm$ symmetry.³⁶ To distinguish these possibilities UV-investigations of dilute solutions as well as thin films of compounds **F8-1/9** and **F6-4/4** were performed. In dilute solution (10^{-4} mol/L in CH_2Cl_2) there is only one peak with a maximum at 287 nm for **F8-1/9** and at 288 nm for **F6-4/4**. In the thin films obtained after spin-coating from THF solution (thickness about $1\text{ }\mu\text{m}$) the absorption is blue-shifted to 266 nm for **F6-4/4** and to 269 nm for compound **F8-1/9** and for both compounds the peak is broadened (Figure S8 in SI). This hypsochromic shift indicates the formation of H-aggregates (there is nearly no fluorescence which is in line with formation of H-aggregates) in which the biphenyls are packed in a molecular arrangement with the transition moments aligned parallel to each other but perpendicular to the line joining their centers (face-to-face arrangement). This confirms the stacking of the aromatics along the cylinder walls in both cases. For **F6-4/4** the hypsochromic shift is stronger ($\Delta\lambda = 22\text{ nm}$) than for **F8-1/9** ($\Delta\lambda = 18\text{ nm}$), which indicates that there are larger aggregates of the aromatics in the case of **F6-4/4** than for **F8-1/9**. This is in accordance with the

proposed models; for F6-4/4 with symmetric distribution of the spacers there is a nearly uninterrupted packing of the biphenyls along the cylinder walls, whereas for compounds with a nonsymmetric distribution of the spacers (F8-1/9 and F6-1/9) there are smaller side-by-side aggregates of the biphenyls along the cylinder walls, and the aggregates of the aromatics are interrupted by parts of the walls formed by the aliphatic spacers. This leads to an averaging of core orientation which is in line with the $p4mm$ symmetry recorded for the mesophases of compounds F8-1/9 and F6-1/9. In line with this model based on local segregation and long-range averaging, also mesophase stability of F6-1/9, as judged by the isotropization temperature, is not reduced if compared with compound F6-4/4. Remarkably, compound F6-4/4, symmetric regarding the spacers (see Figure 5e) and therefore not having this kind of packing issue, even has a significantly reduced mesophase stability compared to F6-1/9 with the same degree of fluorination. The increased stability of the $\text{Col}_{\text{sq}}/p4mm$ phase of F6-1/9 is in line with its more efficient molecular packing and smaller cell size. Thus, it seems that it is favorable for the molecules to have one long rather than two shorter spacers of equal combined length. This effect of the distribution of the spacer on phase stability could to some extent also be due to the different chemical structures of the polar groups in these two compounds. Compound F6-1/9 has a glycerol group at one end providing a higher polarity and one more hydrogen bonding acceptor site than the diol group which is attached to a long aliphatic spacer. The symmetric compound F6-4/4 has both diol groups attached to aliphatic spacers, leading to weaker segregation and reduced hydrogen bonding density which reduces the phase stability.

2.4. Compounds F8- n_1/n_2 . The effect of enlargement of the fluorinated segment in the lateral chain is 2-fold: (i) the stability of the $\text{Col}_{\text{sq}}/p4mm$ phase is increased, as judged by the increased temperature of isotropization (compare F6-1/9 and F8-1/9 in Table 1); (ii) if the phase changes, the new phase comprises cylinders with a larger number of sides (compare F6-1/4 and F8-1/4 in Table 1). The increasing stability of the $p4mm$ phase can be attributed to the enhanced fluorophobic effect which strengthens segregation. However, it is also informative to compare the electron density maps of F6- m/n and F8- m/n compounds that form the common $p4mm$ phase.³⁷ The map of compound F6-4/4 displays only one central maximum; see Figures 5c and S1a (SI). On the other hand, the map for F8-1/9 has a second maximum at the corners of the square cylinder (marked C in Figure 5d; see also Figure S1b in SI). This second maximum is related to the strong (11) Bragg reflections (see Figure 5b and Figure S7c,d in SI). It arises from clustering of the relatively electron-dense glycerol and diol groups at the apexes of the square section of the column. Molecular simulation shows these clusters clearly in compound F8-1/9 (Figure 5f—note the clusters of red oxygens) but not so clearly in compound F6-4/4 (see Figure 5e). Inspection of the molecular models suggests that the bolaamphiphilic molecular backbones in compound F6-4/4 are crumpled, resulting in many broken H-bonds. Most likely this is in order to partially compensate for the deficit in volume of the relatively short lateral semiperfluorinated chain. Thus, it would appear that some molecules forego H-bonding with adjacent head groups and instead have their backbones participate in partially filling the excess free volume inside the cylinder. This option is facilitated by the opportunity to form hydrogen bonds with the ether oxygens at the aromatic cores. This reduces the polar group clustering (nanosegregation) and hence the phase

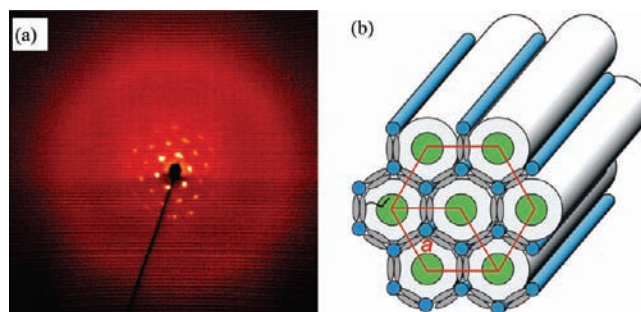


Figure 6. (a) X-ray diffraction pattern of an aligned sample of compound F8-1/4 at $T = 110\text{ }^\circ\text{C}$ (for more details see Table S1 and Figure S6 in SI); (b) model showing molecular organization in the hexagonal honeycomb LC phase (the biphenyl core together with the spacer units is shown as a gray rod).

stability.¹⁴ By contrast, in F8-1/9 that has a larger side chain, the cell interior of the $p4mm$ honeycomb is filled more densely; hence, the molecular cores can stretch, allowing their polar end groups to cluster and increase the phase stability (see Figure 5f). Consistent with the above is the significant increase in lattice parameter from $a_{\text{sq}} = 2.9\text{ nm}$ for F6-1/9 to $a_{\text{sq}} = 3.2\text{ nm}$ for F8-1/9. Such variation in cell parameter is quite unusual for polygonal cylinder phases, where the cell size is fixed by the length of the aromatic core.¹⁵

It is interesting that the diffraction pattern of the $p4mm$ phase formed by compound F6-1/9 has the same weak (11) Bragg reflection (Figure S3d in SI), as observed for compound F6-4/4. This indicates a uniform electron density at the corners of the square cylinder and hence a lack of clustering of the polar groups. Thus, it appears that the R_F chain length, i.e. the space filling inside the cells, is more important for segregation of the polar groups than the kind of distribution of the aliphatic spacers along the backbone.

Increasing the ratio of the lateral chain volume to the length of the molecular backbone beyond that fitting a square honeycomb results in cylinders with a larger number of sides. The columnar mesophases of compounds F8-4/1 and F8-1/4 were confirmed as hexagonal by the observed $1:\sqrt{3}:2$ ratio of reciprocal X-ray d -spacings (Tables S1 in SI). The XRD pattern of an aligned sample of compound F8-1/4, shown as an example in Figure 6a, confirms hexagonal symmetry. The hexagonal lattice parameters for compounds F8-4/1 and F8-1/4 ($a_{\text{hex}} = 4.1\text{ nm}$) agree well with the expected value $a_{\text{hex}} = \sqrt{3}L_{\text{mol}} = 4.3\text{ nm}$, where $L_{\text{mol}} = 2.5\text{ nm}$ is the molecular length. Together with the negative birefringence of the Col_{hex} phase and its optical uniaxiality (see Figure S6c,d in SI), this confirms the hexagonal honeycomb structures for the Col_{hex} phase of compounds F8-4/1 and F8-1/4 (Figure 6b). The number of molecules within a unit cell with an assumed height of $h = 0.45\text{ nm}$ is around 6; hence, the calculated wall thickness is about two molecules, again in agreement with values found for other cylinder phases of T-shaped amphiphiles. The present is thus the same hexagonal honeycomb phase as previously reported for compounds F6-1/1 and F8-1/1 that contained no distinct spacer units, as the single CH_2 groups ($n_1, n_2 = 1$) can be considered as belonging to the polar glycerol groups.¹³

As expected, the hexagonal lattice parameters of the two isomeric compounds F8-4/1 and F8-1/4, differing in the position of the spacer unit relative to the side chain, are very similar. However, there is a relatively large difference in mesophase stability between these two compounds, for F8-1/4 being 21 K

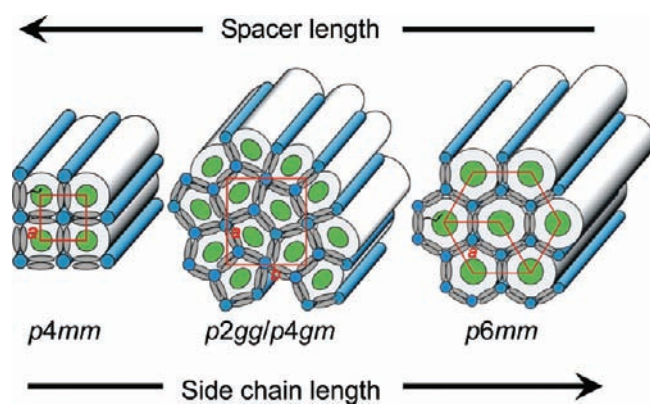


Figure 7. Phase sequence of distinct polygonal cylinder phases, depending on the length of the lateral chains and the total length of the spacer units $n_1 + n_2$.

higher than for **F8-4/1**, see Table 1. It seems that placing the longer spacer beside the lateral chain is favorable for mesophase formation. This effect of the spacer position might also be compared to the reduced mesophase stability of the Col_{squ} phase of compound **F6-4/4** compared to that of compound **F6-1/9**, as discussed in the previous section. Hence, for the self-assembly in LC cylinder phases it seems to be advantageous to have molecules with the longer spacer adjacent to the lateral chain. It is probable that the effect is due to the compatibility between the alkyl segments of the lateral chains and the adjacent backbone alkyl spacers.

3. SUMMARY

T-shaped bolaamphiphiles composed of a biphenyl core, a semiperfluorinated lateral chain, and aliphatic spacer units (n_1, n_2) introduced between the rigid core and the polar groups have been synthesized and investigated by DSC, polarizing microscopy, and XRD. Suggested phase structures are based on XRD patterns, electron density reconstruction, simulations, and investigation of the influence of structural modifications on observed phase types. Four different columnar phases ($\text{Col}_{\text{hex}}/p6mm$, $\text{Col}_{\text{rec}}/p2gg$, $\text{Col}_{\text{squ}}/p4gm$, and $\text{Col}_{\text{squ}}/p4mm$) were found in T-shaped bolaamphiphiles **Fm- n_1/n_2** by increasing the length of aliphatic spacer units n_1, n_2 . These LC phases represent polygonal cylinder phases where the aromatic cores together with the aliphatic spacers make up the walls of polygonal honeycombs fused at the edges by the hydrogen-bonding diol groups and enclosing cells filled by the semiperfluorinated lateral chains. In the observed phase sequence, with increasing overall length of the backbone spacers the cross section of the polygonal honeycomb cells changes from hexagon via pentagon to square (Figure 7). This sequence is in line with the decreasing area-to-circumference ratio achieved by extending the bolaamphiphilic cores.

By introduction of the aliphatic spacers the phase symmetry is enhanced; for example the rhombic cylinder phase, typically observed for related biphenyl-based compounds without spacers and with appropriate side-chain length (compounds **Fm-1/1**, Figure 1c), is replaced by the square cylinder phase with higher symmetry. Likewise, there is a tendency to form the square $p4gm$ lattice rather than the less symmetric rectangular $p2gg$ lattice for pentagonal honeycombs, as indicated by the $p2gg - p4gm$ transition in compound **F6-1/4**. It is most likely that the more central position of the alkyl chains at the bolaamphiphilic core reduces restrictions in chain packing, thereby allowing the system

to adopt the lattice with the highest possible symmetry. Alternatively, the higher symmetry may merely be due to increasing entropy-driven disorder, facilitated by higher molecular flexibility, as discussed above.

Interestingly, even rather long spacer units can retain the molecular self-assembly in honeycomblike structures, although the cylinder walls become more flexible. These aliphatic spacers provide additional flexibility to these structures which allows a specific type of cylinder structure to tolerate a broader range of lateral chain volumes by enabling some expansion/compression of the honeycombs. The electron density maps suggest that such adjustment may occur at the expense of some hydrogen bonding. Formation of certain cylinder walls by aliphatic chains instead of aromatic cores was previously reported for the trapezoid cylinder phase formed by some T-shaped facial amphiphiles.³⁸ However, in that case the alkyl chains form walls of their own, free of the aromatic moiety.

Although the change of the cylinder shape is principally the same as observed by elongation of the π -conjugated rigid core, the effect of spacer elongation on the phase transition temperatures is reversed. Whereas elongation of a linear and rigid moiety dramatically increases both melting and clearing temperatures,²¹ backbone extension by alkyl spacers reduces the clearing temperatures without influencing the melting temperatures significantly. Thus, replacing parts of the aromatic cores by flexible units is an appropriate tool for increasing the size of the polygonal honeycombs without moving the transitions to unfavorably high temperature ranges.

In summary, extension of the bolaamphiphilic core by flexible spacer units can be used to increase the size of the polygonal cylinders, to achieve larger periodicities and to increase the symmetry of the self-assembled liquid-crystalline honeycombs.

■ ASSOCIATED CONTENT

S Supporting Information. Synthesis procedures and analytical data, additional DSCs, textures and XRD data. This material is available free of charge via the Internet at <http://pubs.acs.org>.

■ AUTHOR INFORMATION

Corresponding Author

xhcheng@ynu.edu.cn; carsten.tschierske@chemie.uni-halle.de; g.ungar@sheffield.ac.uk

■ ACKNOWLEDGMENT

This work was supported by the National Natural Science Foundation of China (No. 21074105 and No. 20973133), the Yunnan Science Foundation (2010CD018). M.P. acknowledges the support by the Cluster of Excellence “Nanostructured Materials” and DFG (FG 1145). G.U. also acknowledges the support from the WCU program through the National Research Foundation of Korea funded by the Ministry of Education, Science and Technology (R31-10013). For help with the synchrotron experiments we thank Drs. Nick Terrill and Jen Hiller (beamline I22) of the Diamond Light Source, U.K.

■ REFERENCES

(1) (a) Steed, J. W.; Atwood, J. L. *Encyclopedia of Supramolecular Chemistry*; Marcel Dekker: New York, 2004. (b) Lehn, J. M. *Supramolecular Chemistry*; Wiley-VCH: Weinheim, Germany, 1995.

- (2) (a) Collings, P. J.; Hird, M. *Introduction to Liquid Crystals*; Taylor & Francis: London, 1997. (b) Demus, D.; Goodby, J.; Gray, G. W.; Spiess, H.-W.; Vill, V. *Handbook of Liquid Crystals*; Wiley-VCH: Weinheim, Germany, 1998, Vol. 1–3. (c) Pauluth, D.; Tarumi, K. *J. Mater. Chem.* **2004**, *14*, 1219–1227.
- (3) (a) Kato, T.; Mizoshita, N.; Kishimoto, K. *Angew. Chem., Int. Ed.* **2006**, *45*, 38–68. (b) Saez, I. M.; Goodby, J. W. *J. Mater. Chem.* **2005**, *15*, 26–40. (c) Ungar, G.; Zeng, X. *Soft Matter.* **2005**, *1*, 95–106. (d) Laschat, S.; Baro, A.; Steinke, N.; Giesselmann, F.; Hägele, C.; Scalia, G.; Judele, R.; Kapatsina, E.; Sauer, S.; Schreivogel, A.; Tosoni, M. *Angew. Chem., Int. Ed.* **2007**, *46*, 4832–4887. (e) Lee, M.; Cho, B.-K.; Zin, W.-C. *Chem. Rev.* **2001**, *101*, 3869–3892.
- (4) (a) Ringsdorf, H.; Scharlb, B.; Venzmer, J. *Angew. Chem., Int. Ed.* **1988**, *27*, 113–158. (b) Greig, L. M.; Philp, D. *Chem. Soc. Rev.* **2001**, *30*, 287–302. (c) Lehn, J.-M. *Proc. Natl. Acad. Sci. U.S.A.* **2002**, *99*, 4763–4768. (d) Hoeben, F. J. M.; Jonkheijm, P.; Meijer, E. W.; Schenning, A. P. H. J. *Chem. Rev.* **2005**, *105*, 1491–1546. (e) Keizer, H. M.; Sijbesma, R. P. *Chem. Soc. Rev.* **2005**, *34*, 226–234.
- (5) Rosen, B. M.; Wilson, C. J.; Wilson, D. A.; Peterca, M.; Imam, M. R.; Percec, V. *Chem. Rev.* **2009**, *109*, 6275–6540.
- (6) (a) Donnio, B.; Guillon, D. *Adv. Polym. Sci.* **2006**, *201*, 45–155. (b) Lenoble, J.; Campidelli, S.; Maringa, N.; Donnio, B.; Guillon, D.; Yevlampieva, N.; Deschenaux, R. *J. Am. Chem. Soc.* **2007**, *129*, 9941–9952.
- (7) (a) Baranoff, E. D.; Voignier, J.; Yasuda, T.; Heitz, V.; Sauvage, J.-P.; Kato, T. *Angew. Chem., Int. Ed.* **2007**, *46*, 4680–4683. (b) Aprahamian, I.; Yasuda, T.; Ikeda, T.; Saha, S.; Dichtel, W. R.; Isoda, K.; Kato, T.; Stoddart, J. F. *Angew. Chem., Int. Ed.* **2007**, *46*, 4675–4679.
- (8) Kitzerow, H.-S.; Bahr, C. *Chirality in Liquid Crystals*; Springer: New York, 2001; Pansu, B. *Mod. Phys. Lett. B* **1999**, *13*, 769–782.
- (9) (a) Reddy, R. A.; Tschierske, C. *J. Mater. Chem.* **2006**, *16*, 907–961. (b) Takezoe, H.; Takanishi, Y. *Jpn. J. Appl. Phys.* **2006**, *45*, 597–625.
- (10) (a) Ikuma, N.; Tamura, R.; Shimono, S.; Kawame, N.; Tamada, O.; Sakai, N.; Yamauchi, J.; Yamamoto, Y. *Angew. Chem., Int. Ed.* **2004**, *43*, 3767–3682. (b) Zienkiewicz, J.; Fryszkowska, A.; Zienkiewicz, K.; Guo, F.; Kaszynski, P.; Januszko, A.; Jones, D. *J. Org. Chem.* **2007**, *72*, 3510–3520. (c) Terazzi, E.; Bourgogne, C.; Welter, R.; Gallani, J.-L.; Guillon, D.; Rogez, G.; Donnio, B. *Angew. Chem., Int. Ed.* **2008**, *47*, 490–495.
- (11) Zeng, X.; Ungar, G.; Liu, Y.; Percec, V.; Dulcey, A. E.; Hobbs, J. K. *Nature* **2004**, *428*, 157–160.
- (12) Kölbl, M.; Beyersdorff, T.; Cheng, X. H.; Tschierske, C.; Kain, J.; Diele, S. *J. Am. Chem. Soc.* **2001**, *123*, 6809–6818.
- (13) Cheng, X. H.; Prehm, M.; Das, M. K.; Kain, J.; Baumeister, U.; Diele, S.; Leine, D.; Blume, A.; Tschierske, C. *J. Am. Chem. Soc.* **2003**, *125*, 10977–10996.
- (14) (a) Tschierske, C. *J. Mater. Chem.* **1998**, *8*, 1485–1508. (b) Tschierske, C. *J. Mater. Chem.* **2001**, *11*, 2647–2671. (c) Tschierske, C. *Ann. Rep. Progr. Chem. Ser. C.* **2001**, *97*, 168–191. (d) Tschierske, C. *Curr. Opin. Colloid Interface Sci.* **2002**, *7*, 69–80.
- (15) Tschierske, C. *Chem. Soc. Rev.* **2007**, *36*, 1930–1970.
- (16) Glettner, B.; Liu, F.; Zeng, X.; Prehm, M.; Baumeister, U.; Bates, M. A.; Walker, M.; Boesecke, P.; Ungar, G.; Tschierske, C. *Angew. Chem., Int. Ed.* **2008**, *47*, 9063–9066.
- (17) (a) Cheng, X. H.; Das, M. K.; Baumeister, U.; Diele, S.; Tschierske, C. *J. Am. Chem. Soc.* **2004**, *126*, 12930–12940. (b) Prehm, M.; Liu, F.; Baumeister, U.; Zeng, X. -B.; Ungar, G.; Tschierske, C. *Angew. Chem., Int. Ed.* **2007**, *46*, 7972–7975.
- (18) (a) Chen, B.; Baumeister, U.; Diele, S.; Das, M. K.; Zeng, X.-B.; Ungar, G.; Tschierske, C. *J. Am. Chem. Soc.* **2004**, *126*, 8608–8609. (b) Chen, B.; Zeng, X.-B.; Baumeister, U.; Diele, S.; Ungar, G.; Tschierske, C. *Angew. Chem., Int. Ed.* **2004**, *43*, 4621–4625. (c) Chen, B.; Zeng, X.-B.; Baumeister, U.; Ungar, G.; Tschierske, C. *Science* **2005**, *307*, 96–99. (d) Chen, B.; Baumeister, U.; Pelzl, G.; Das, M. K.; Zeng, X.-B.; Diele, S.; Ungar, G.; Tschierske, C. *J. Am. Chem. Soc.* **2005**, *127*, 16578–16591. (e) Liu, F.; Chen, B.; Baumeister, U.; Zeng, X.; Ungar, G.; Tschierske, C. *J. Am. Chem. Soc.* **2007**, *129*, 9578–9579.
- (19) (a) Prehm, M.; Liu, F.; Zeng, X.-B.; Ungar, G.; Tschierske, C. *Angew. Chem., Int. Ed.* **2007**, *46*, 7972–7975. (b) Prehm, M.; Enders, C.; Anzahae, M. Y.; Glettner, B.; Baumeister, U.; Tschierske, C. *Chem.—Eur. J.* **2008**, *14*, 6352–6368. (c) Kieffer, R.; Prehm, M.; Pelz, K.; Baumeister, U.; Liu, F.; Hahn, H.; Lang, H.; Ungar, G.; Tschierske, C. *Soft Matter* **2009**, *5*, 1214–1227.
- (20) (a) Cheng, X. H.; Das, M. K.; Diele, S.; Tschierske, C. *Angew. Chem., Int. Ed.* **2002**, *41*, 4031–4035. (b) Prehm, M.; Cheng, X. H.; Diele, S.; Das, M. K.; Tschierske, C. *J. Am. Chem. Soc.* **2002**, *124*, 12072–12073. (c) Prehm, M.; Diele, S.; Das, M. K.; Tschierske, C. *J. Am. Chem. Soc.* **2003**, *125*, 614–615. (d) Patel, N. M.; Dodge, M. R.; Zhu, M. H.; Petschek, R. G.; Rosenblatt, C.; Prehm, M.; Tschierske, C. *Phys. Rev. Lett.* **2004**, *92*, 015501. (e) Patel, N. M.; Syed, I. M.; Rosenblatt, C.; Prehm, M.; Tschierske, C. *Liq. Cryst.* **2005**, *32*, 55–61.
- (21) See, for example, compound D in: Kieffer, R.; Prehm, M.; Glettner, B.; Pelz, K.; Baumeister, U.; Liu, F.; Zeng, X.-B.; Ungar, G.; Tschierske, C. *Chem. Commun.* **2008**, 3861–3863.
- (22) Cheng, X. H.; Dong, X.; Huang, R.; Zeng, X.-B.; Ungar, G.; Prehm, M.; Tschierske, C. *Chem. Mater.* **2008**, *20*, 4729–4738.
- (23) Cheng, X. H.; Dong, X.; Wei, G.; Prehm, M.; Tschierske, C. *Angew. Chem., Int. Ed.* **2009**, *48*, 8014–8017.
- (24) Prehm, M.; Götz, G.; Bäuerle, P.; Liu, F.; Ungar, G.; Tschierske, C. *Angew. Chem., Int. Ed.* **2007**, *46*, 7856–7859.
- (25) A monotropic phase assigned as Col_{qu}/p4mm in ref 13 (compound F4-1/1) turned out to be actually a 3D-hexagonal phase: Liu, F.; Zeng, X.; Ungar, G.; Tschierske, C. unpublished results.
- (26) (a) Miyaura, N.; Yanagi, T.; Suzuki, A. *Synth. Commun.* **1981**, *11*, 513–519. (b) Hird, M.; Gray, G. W.; Toyne, K. J. *Mol. Cryst. Liq. Cryst.* **1991**, *206*, 187–204. (c) Miyaura, N.; Suzuki, A. *Chem. Rev.* **1995**, *95*, 2457–2483.
- (27) Chen, Q.-Y.; Yang, Z. Y.; Zhao, C.-X.; Qiu, Z. M. *J. Chem. Soc., Perkin Trans. 1* **1988**, 563–567.
- (28) Majetch, G.; Hicks, R.; Reister, S. *J. Org. Chem.* **1997**, *62*, 4321–4326.
- (29) Yamoto, Y.; Hatsuya, S.; Yamada, J. *J. Org. Chem.* **1990**, *55*, 3118–3128.
- (30) Kitamura, M.; Isobe, M.; Ichikawa, Y.; Goto, T. *J. Am. Chem. Soc.* **1984**, *106*, 3252–3257.
- (31) Van Rheenen, V.; Cha, D. Y.; Hartley, W. M. *Org. Synth.* **1979**, *58*, 43–51.
- (32) Kölbl, M.; Beyersdorff, T.; Tschierske, C.; Diele, S.; Kain, J. *Chem.—Eur. J.* **2000**, *6*, 3821–3837.
- (33) Immirzi, A.; Perini, B. *Acta Crystallogr., Sect. A.* **1977**, *33*, 216–218.
- (34) That the biphenyl cores are oriented perpendicular to the column axis is shown by the color of the fans in the optical micrographs (Figures 3c,d, and 4b, Figures S4d, S6d, S7g in SI) taken with a λ -plate. The yellow and blue colors define the orientation of the high-index axis as radial rather than tangential. Since the columns are tangential in the fans, and the high-index axis is known to be parallel to the biphenyl long axis, it follows that the biphenyls are perpendicular to the columns; ($n_{\parallel} < n_{\perp}$ = optically negative).
- (35) The value $h = 0.45$ nm was used in all calculations, independent of the actual position of the maximum of the wide angle scattering in the diffraction pattern. The reason is that the bolaamphiphilic units (their average diameter is 0.45 nm) are responsible for the lattice of the cylinder shells, whereas the semiperfluoralkyl chains only fill the channels within this structure. Because the cross section of the perfluorinated segments is larger than the rest of the molecules, there is a drift of the maximum of the diffuse scattering in the X-ray diffraction pattern to larger d -values with increasing degree of fluorination. However, this shift is due to a change of a molecular parameter rather than due to a change of the structure. Because the diameter of the fluorinated segments is larger than that of the nonfluorinated bolaamphiphilic moieties, which form the cylinder walls, there is a mixing of the chains of adjacent (hypothetical) unit cells along the cylinders, i.e. the perfluorinated chains in one (hypothetical) unit cell also contribute to the space filling in the adjacent unit cell.

(36) A nonsegregated antiparallel packing of the bolaamphiphilic cores in the cylinder walls could become possible if steric and packing effects are dominant over the segregation between biphenyl and alkylene spacers (see: Lose, D.; Diele, S.; Pelzl, G.; Dietzmann, E.; Weissflog, W. *Liq. Cryst.* **1998**, *24*, 707–717. Pensec, S.; Tourmilhac, F.-G.; Bassoul, P.; Durliat, C. *J. Phys. Chem. B* **1998**, *102*, 52–60). However, as the cross-sectional area of alkyl chains and biphenyl cores is nearly equal, a randomly mixed structure becomes unlikely for compounds $1/n-1/9$, as confirmed by the investigation of UV absorption; alternation of blocks with different core orientations along the cylinder walls could remove small differences in packing of the biphenyls and alkylene spacers.

(37) Increasing the length of the high electron density R_F chains from $n = 6$ to $n = 8$ (compounds **F6-4/4**, **F8-1/9**) by retaining the $p4mm$ lattice leads to an expansion of the high electron density regions in the centers of the low electron density continuum in the electron density maps (see Figure 5c,d); hence, the phase choice must be correct, as expansion of the high electron density units leads to an increase of the high electron density areas. In this way inverted phase structures could be excluded.

(38) Liu, F.; Chen, B.; Glettner, B.; Prehm, M.; Das, M. K.; Baumeister, U.; Zeng, X. -B; Ungar, G.; Tschierske, C. *J. Am. Chem. Soc.* **2008**, *130*, 9666–9667.